3177

To be published in Central Laser Facility, Annual Report 2004-05, Rutherford Appeton Laboratory, U.K

Light-Induced Domain Engineering in Ferroelectrics

C.L. Sones, C.E.Valdivia, J.G.Scott, S. Mailis, R.W.Eason
Optoelectronics Research Centre, University of Southampton, Highfield, Southampton, SO17 1TW, U.K
D.A. Scrymgeour, V. Gopalan
Materials Research Laboratory, Pennsylvania State University, University Park, PA, 16802, U.S.A
T. Jungk, E. Soergel
Institute of Physics, University of Bonn, Wegelerstr. 8, 53115 Bonn, Germany
I.P. Clark
CCLRC Rutherford Appleton Laboratory, Chilton, Didcot, Oxfordshire, OX11 0QX, U.K

Main contact email address: cls@orc.soton.ac.uk

Introduction

Fabrication of periodically inverted domain patterns in ferroelectric materials such as lithium niobate has been widely researched for the realisation of applications as diverse as quasi-phase-matched (QPM) non-linear devices, electro-optic Bragg deflectors, photonic band-gap structures, and piezoelectric devices such as micro-resonators, atom traps and micro-cavities.

While several techniques such as Li_2O out-diffusion[1)], proton-exchange followed by heat treatment[2)], Ti-indiffusion[3)], scanning force microscopy[4)], e-beams[5-6)] and electric field poling[7)] have been successfully demonstrated for achieving domain inversion over the past years, even perhaps the most routinely used technique of electric-field-induced domain inversion (E-field poling) becomes problematic when periodicities of a few microns and below are desired for first-order QPM non-linear processes.

In order to overcome the limitations associated with E-field poling, we have been investigating the feasibility of a relatively simple single-step technique, which exploits the interaction of intense laser light with ferroelectric lithium niobate to engineer domains at micron and sub-micron scale-lengths. Some light-assisted poling experiments which take advantage of the ultraviolet light-induced transient change in the coercive field of the illuminated ferroelectric material to transfer a patterned light distribution into an equivalent domain structure in bulk crystals have already been reported for lithium tantalate[8-9)] and lithium niobate[10-11)] crystals. In this letter we report a direct *optical poling* technique that employs pulsed ultraviolet laser light to induce surface domain inversion in undoped lithium niobate in a single step. We further characterize the laser modified domain manipulated crystals using differential chemical etching and scanning force microscopy (SFM).

Experiments and results

To investigate the effects of controlled exposure in near surface region, the laser wavelengths (between 298 nm and 329 nm) we have chosen to explore straddle the UV absorption edge of lithium niobate for which the transmission starts to increase as we approach 300 nm. Laser illumination at these wavelengths was through the NSL-4 laser available at the LSF of the RAL, and consisted of frequency-doubled Q-switched Nd:YAG laser (Continuum Powerlite 8000) pumping a frequency-doubled dye laser (Sirah PrecisionScan), generating mJ level pulses between 298 nm and 329 nm (~7-ns pulses). For both laser systems, the beam passed through an aperture to select a small region of improved spatial uniformity and this area was subsequently imaged onto the +z face of a 500-μm thick single crystal congruent lithium niobate sample (Crystal Technology, USA).

For incident energy densities near the single-pulse ablation threshold of lithium niobate (of order 0.5 J cm^{-2}), uniform UV irradiation produces little surface damage. As energy densities increase however, multiple pulse exposures of 5 pulses of 298-nm light at an energy density per pulse of ~10 J cm^{-2} leads to ablation depths of ~1.5 μm. Interestingly, the wide range of fluences (~0.5-10 J cm^{-2}) tested at 298 nm, produce similar results when examined by both selective etching and SFM (discussed below), providing a broad processing window for this direct optical poling effect.

Following exposure of the +z crystal faces, the irradiated lithium niobate samples were etched at room temperature for 30-60 minutes in hydrofluoric (HF) acid, which is well known to selectively etch the –z crystalline face, with no effect on the +z face. Scanning electron microscopy (SEM) images of the resulting structures on the +z face show within the UV-irradiated regions a self-organized pattern of etched trenches (FIG. 1(a)) that run parallel and at $\pm 60^0$ angles to the crystallographic y-axis, indicating that their formation is dictated by the underlying 3m crystal symmetry. The inset in FIG. 1(a) shows the 2-D Fourier transform, confirming that growth occurs along these crystalline directions only. Analysis of all the SEM micrographs showed that the trenches illustrated by FIG. 1(b) had widths that fell within the range of 150-300 nm, with most line features uniform along their lengths. The longest lines, extending up to hundreds of microns, were seemingly limited only by the spot size of the UV beam incident on the sample surface. FIG. 1(b) shows a close-up of one of these pulsed UV laser-induced line features, and it is clear that the trench is small (~160-nm width), highly uniform, straight and has been etched out of the surrounding +z face, indicating the likely presence of a –z oriented domain feature.

The depth of these trenches was evaluated by further HF etching, followed by focused ion beam (FIB) milling. As the etch rate of the –z face of lithium niobate in 48% HF solution is ~0.8 μm hr^{-1} at room temperature[12)], further etching was undertaken for 18 hours to ensure that the maximum etch depth had been reached. Sideways etching also occurs over this length of time, producing broadening of the trench width so that the FIB-measured widths of ~400 nm do not necessarily reflect the minimum widths of these features.

Following etching, a channel was milled across the trenches, depicted in FIG. 2(a), using an FIB (FEI, Bristol, UK). The same FIB was used to image the milled channel at an angle of 45^0, shown in FIG. 2(b). From this close-

up view of the cross-sectional depth of the trench features, it is apparent that they extend to a depth approaching 2 μm. A comparison can be made here between these triangular shaped features and electric-field periodically poled surface domains seen via y-face etching studies, which extend to depths of order 10 μm[13-14]. The close similarity suggests that these etched trenches indicate that UV illumination has induced domain-inverted material (–z orientation) within the background +z face.

For wavelengths shorter than 300 nm, the transmission of light through a 500-μm thick sample of lithium niobate is effectively zero, while the 50% transmission point occurs for a value of 328 nm. Though irradiation of the +z face was undertaken at many different wavelengths, the features revealed by the selective chemical etching, however, were only observed for the wavelength range of 298-306 nm. For wavelengths longer than 306 nm, it is possible that similar patterns would appear on the surface of the crystals for higher incident laser fluences, but these were not apparent up to the maximum fluences used of 7 J cm^{-2} per pulse in our studies.

At least a small amount of surface ablation by the incident laser light appeared to be a prerequisite for the formation of these self-organized features. In cases where no ablation appeared, HF acid treatment has not been observed to reveal the self-organized patterns. This may indicate a possible mechanism for the formation of these features, such as Li_2O out-diffusion induced by the local surface heating from the absorbed light. It may also be possible that the reaction force from the ablated material onto the surface of the crystal substrate produces a local electric field through the piezoelectric effect that assists the formation of domains at an elevated temperature. This domain nucleation is likely to initiate at structural defects and propagate along crystalline directions, forming the lines seen in FIG. 1.

To further elucidate the nature of these features, the well-established approach of scanning force microscopy (SFM), routinely employed in the visualisation of ferroelectric domains, and well-suited for conclusively distinguishing between anti-parallel domain orientations was employed. Imaging oppositely-oriented domains in ferroelectrics is possible by SFM due to their 180^0 phase-shifted response. An SFM was operated in contact mode using a conductive probe tip to apply an A.C. voltage (V_{pp} = 10–20 V, f = 35-38 kHz). A cantilever with a large spring constant (14 N m^{-1}) was used to ensure limited interference from electrostatic effects[15].

The SFM scans of *un-etched* +z face of lithium niobate irradiated with 298 nm light (FIG. 3) show similar patterns to those revealed by selective chemical etching. Topography scans without an applied voltage confirmed that the lines of contrast in FIG. 3 do not correspond to topographical features prior to etching.

Summary

The UV-induced features display contrast in piezoelectric response relative to the surrounding areas and preferential etching compared to the surrounding un-etched +z face. Furthermore, the cross-sectional depth profile is very similar to that of surface domains formed through electric field over-poling. The evidence therefore leads to the conclusion that these line features correspond to near-surface domain-inverted material, induced by interaction of the incident UV light. We believe that this is the first example of direct optical poling through a single-step interaction process.

References

1. K Yamamoto, K Mizuuchi, K Takeshige, Y Sasi, T Taniuchi, J.Appl.Phys, **70(4)**, 1947, (1991).
2. K Nakamura, H Shimizu, Appl.Phys.Lett, **56(16)**, 1535, (1990)
3. S Miyazawa, J.Appl.Phys, **50(7)** ,4599, (1979)
4. K Terabe, M Nakamura, S Takekawa, K Kitamura, S Higuchi, Y Gotoh, Y Cho, Appl.Phys.Lett, **82 (3)**, 433, (2003)
5. M Yamada, K Kishima, Electron.Lett, **27(10)**, 828, (1991).
6. H Ito, C Takyu, H Inaba, Electron.Lett, **27(14)**, 1221, (1991)
7. M Yamada, N Nada, M Saitoh, K Watanabe, Appl.Phys.Lett, **62(5)**, 435, (1993)
8. S Chao, W Davis, D.D Tuschel, R Nichols, M Gupta, H.C Cheng, Appl.Phys.Lett, **67**, 1066, (1995)
9. P.T Brown, G.W Ross, R.W Eason, A.R Pogosyan, Opt.Commun, **163**, 310, (1999)
10. M Müller, E Soergel, K Buse, Appl.Phys.Lett, **83(9)**, 1824, (2003)
11. A Fujimura, T Sohmura, T Suhara, Electron.Lett, **39 (9)**, 719, (2003)
12. C. L. Sones, S. Mailis, W. S. Brocklesby, R. W. Eason, and J. R. Owen, J. Mater. Chem. **12** (2), 295 (2002)
13. A. C. Busacca, C. L. Sones, V. Apostolopoulos, R. W. Eason, and S. Mailis, Appl. Phys. Lett. **81** (26), 4946 (2002)
14. C. L. Sones, University of Southampton, 2003.
15. G. Hu, T. Tang, and J. Xu, Jpn. J. Appl. Phys. **41** (1, 11B), 6793 (2002)

Figure Captions

FIG1: SEM micrographs of the +z face of lithium niobate exposed to 298-nm light (~0.7 J cm^{-2}, 5 pulses) and subsequently etched in HF acid for 30 minutes. (a) Etched trenches aligned parallel and at $\pm 60^0$ to the y-axis (vertical). Inset shows the 2D Fourier transform of the etched pattern, clearly demonstrating the 3-fold symmetry. (b) Detail from (a), showing a single continuous etched line feature of good uniformity.

FIG. 2: (a) Diagram of an FIB-milled channel crossing two etched UV-induced trenches. (b) FIB micrograph of a fabricated area, corresponding to the region shown from (a), viewed at a 45^0 angle. The etched trenches are shown to extend to 1.9-μm depths; width broadening is also observable, as compared to the measured widths (150-300 nm) after shorter etch durations. The two trenches, formed by a large-area exposure of 298-nm light (~1.5 J cm^{-2}, 2 pulses), were revealed by selective chemical etching in HF acid for 18 hours.

FIG. 3: SFM scans showing amplitude response following exposure of the +z face to pulsed UV light at wavelengths of 298 nm (3 J cm^{-2}, 5 pulses). The patterns recorded with this imaging.technique are effectively identical to those produced through selective chemical etching followed by SEM imaging (as in FIG. 1).

Figure 1

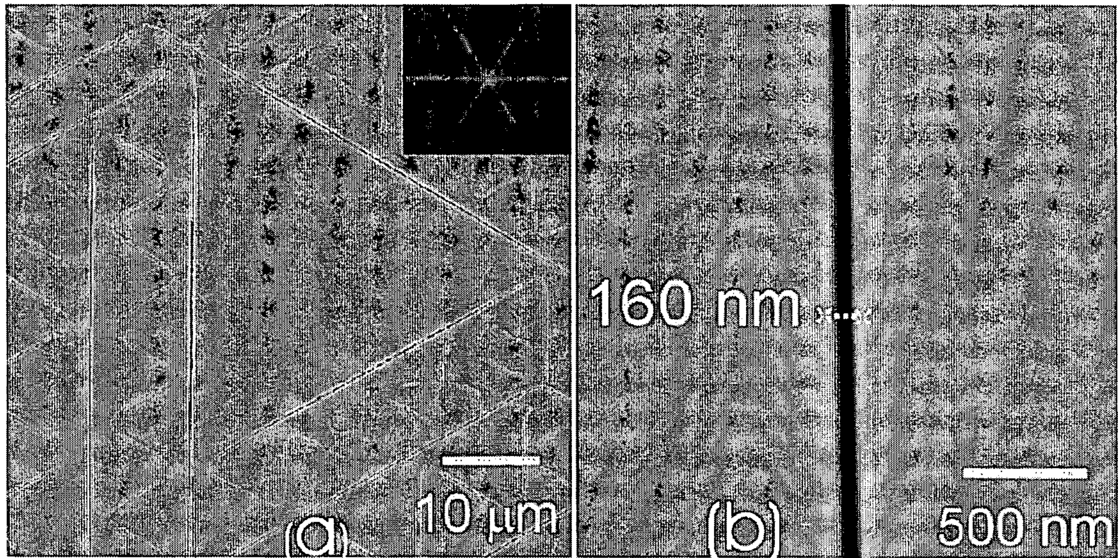

Figure 2

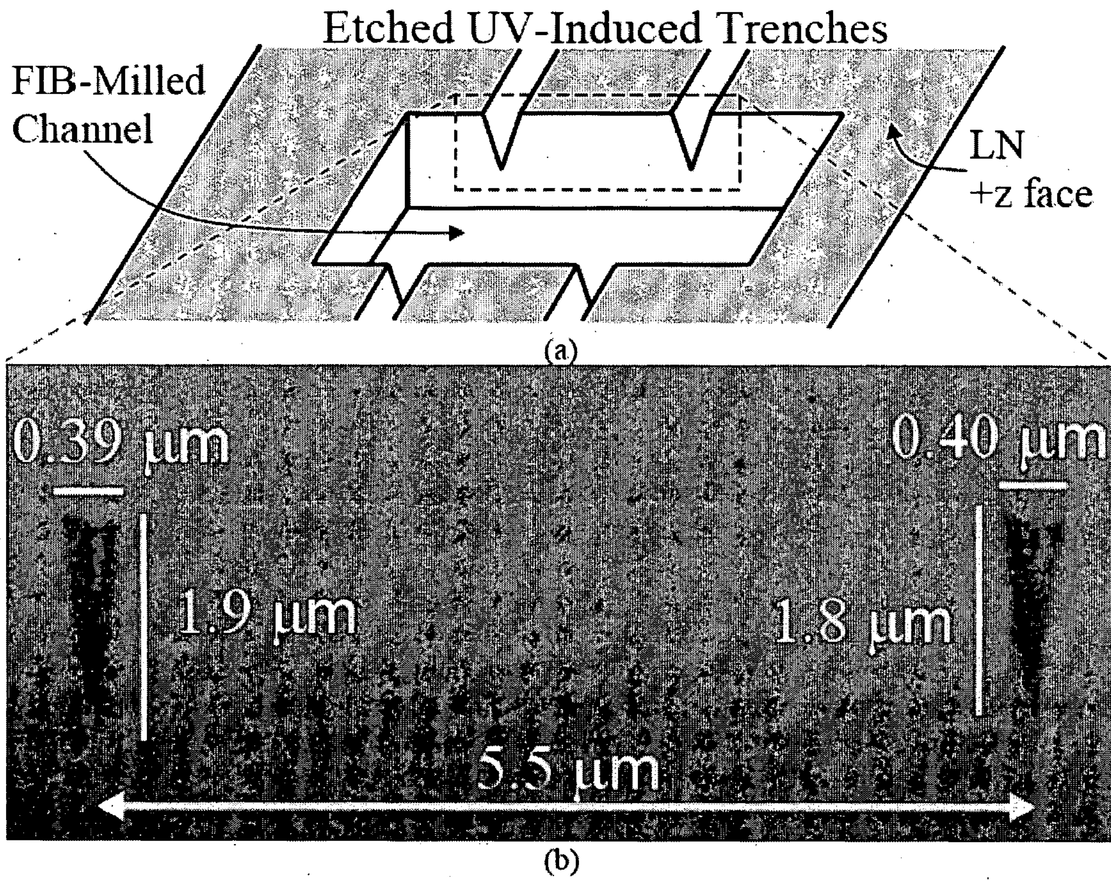

Figure 3